Origins and manufacture of the glass mosaic tesserae from the great Umayyad Mosque in Damascus

Nadine Schibille, Patrice Lehuédé, Isabelle Biron, Léa Brunswic, Étienne Blondeau, Bernard Gratuze

Journal of Archaeological Science 147 (2022) 105675

Contents lists available at ScienceDirect

Journal of Archaeological Science

journal homepage: www.elsevier.com/locate/jas

Origins and manufacture of the glass mosaic tesserae from the great Umayyad Mosque in Damascus

Nadine Schibille [a,*], Patrice Lehuédé [b], Isabelle Biron [b], Léa Brunswic [b,c], Étienne Blondeau [c], Bernard Gratuze [a]

[a] Institut de Recherche sur Les Archéomatériaux, Centre Ernest-Babelon (IRAMAT-CEB), UMR7065, CNRS/Université D'Orléans, 45071, Orléans, France
[b] Centre de Recherche et de Restauration des Musées de France (C2RMF), UMR8247 CNRS-IRCP, 75001, Paris, France
[c] Département des Arts de L'Islam, Musée Du Louvre, 75001, Paris, France

ARTICLE INFO

Keywords:
LA-ICP-MS
Raman spectroscopy
SEM
Islamic glass
Gold analyses
Logistics of supply
Recycling

ABSTRACT

The Great Umayyad Mosque of Damascus built between about 706 and 714/15 CE is the oldest surviving mosque that still preserves large parts of its original architecture and decoration. The origins of the mosaic tesserae have been the subject of debate for more than a thousand years. The earliest sources written two centuries after the construction of the edifice claim a Byzantine origin of both, the material as well as the craftsmen. Here we use the compositional analyses of nearly 1,000 glass tesserae to show that 65% of the samples (80% of the coloured tesserae) from the mosque have a consistent chemistry and, by inference, originate from a common geographical source. Comparison with chemical data of early Islamic glass groups conclusively identifies Egypt as the origin of these tesserae and demonstrates that they are coeval with the foundation of the mosque. Additionally, the compositional features of the gold leaf tesserae testify to the systematic recycling and reuse of older material. Our findings suggest that the manufacture and supply of glass tesserae for the Great Mosque was a direct commission from the highest echelons of government.

1. Introduction

The turn of the 8th century CE was a *Golden Age* of mosaic making in the Islamic world, when within one generation several monumental mosques were built that contained vast surfaces of wall mosaics. By far the largest of these was the Great Umayyad Mosque of Damascus (Finster, 1970; Grafman and Rosen-Ayalon, 1999; James, 2017; Leal, 2020). The Damascene mosque soon became the ultimate architectural model for congregational mosques in Syria and beyond, yet the origins of the mosaic tesserae and what motivated this choice of decoration have been the stuff of legends (Flood, 2001; George, 2021; James, 2017). The mosque's architecture, decoration and even the stories surrounding its creation were copied throughout the medieval Islamic world, from the mosques of Samarra (Iraq) in the east to Córdoba (Spain) in the west (James, 2017; Gómez-Morón et al., 2021). The use of mosaics in early Islamic religious architecture was a politicised decision, one that proclaimed cultural supremacy and identity (Flood, 2001; George, 2021; Gómez-Morón et al., 2021; James, 2017). Islamic textual sources claim that the mosques were designed to surpass the splendour of Byzantine churches, and that the Caliph al-Walid received the materials for the mosaics of the Great Mosque in Damascus from the Byzantine Emperor himself (De Goeje, 2014; El-Cheikh, 2001; Qaddumi, 1996). However, no archaeological evidence of the origin of the mosaic tesserae has thus far been presented, with the exception of a preliminary analysis of 24 tesserae (Fiorentino, 2021). Large sections of the original mosaics survive at the monument (Fig. 1; Finster, 1970), despite repeated destructions and repairs that have resulted in considerable losses (George, 2021). Using approximate values for the size of the tesserae (0.75 cm^3) and the average density of glass tesserae (2.7 g/cm^3), the Great Mosque of Damascus with roughly 7,500 m^2 of mosaic surface (Leal, 2020) would have swallowed of the order of 150 tons of glass. This lavish use of glass means that sufficient resources had to be mobilised, yet the choice of material was far from pragmatic or based on local availability.

Some 1,400 glass tesserae of all colours, including gold and silver leaf samples, now housed in the Islamic Department of the Musée du Louvre in Paris, were collected during the restoration campaign and the partial uncovering of the Barada mosaics in the west arcade at the initiative of Eustache de Lorey during the French Mandate (De Lorey, 1931; George,

* Corresponding author.
E-mail address: nadine.schibille@cnrs.fr (N. Schibille).

https://doi.org/10.1016/j.jas.2022.105675
Received 24 April 2022; Received in revised form 16 August 2022; Accepted 18 September 2022
Available online 24 September 2022

Fig. 1. Mosaic panel from the west arcade of the Umayyad (Great) Mosque in Damascus. © Judith McKenzie/Manar al-Athar Digital Archive, Oxford 2013, available at www.manar-al-athar.ox.ac.uk.

2021). We are unable to pinpoint the exact location within in the building where these tesserae were collected, as the French archives are silent on the issue and the archives in Damascus are not currently accessible. However, judging from Lorey's work and the composition of the material, they are part of the original Umayyad decoration that is primarily concentrated in the west arcade of the mosque. About two thirds of these tesserae (all the loose ones not set in plaster) have been investigated by a combination of different analytical methods to establish the compositional and structural characteristics of the samples and to determine the provenance and manufacturing techniques of the tesserae. Applying optical microscopy, the tesserae were classified into nine major translucent and opaque colour groups exhibiting an almost infinite number of hues (Table S1; Fig. S1). Polished cross-sections of microsamples were prepared from 30 opaque tesserae representative of the different colour groups and choice of hues (except blue) for scanning electron microscopy (SEM-EDS) and Raman spectroscopy to identify different particles and phases contained in the glass. We then conducted laser ablation inductively coupled plasma mass spectrometry (LA-ICP-MS) of all samples to provide a high-resolution chemical characterisation of all major, minor and trace elements. The resulting data were evaluated statistically to ascertain the compositional variability across the assemblage. Comparison of the compositional fingerprints allowed us to identify the likely source of the mosaic tesserae and advance a model of the organisation of mosaic production in the early 8th century.

2. Materials and Methods

2.1. Backscattered images and localized particle analysis in the SEM

To ensure conductivity, the mounted and polished cross-sections of 30 samples were sputtered with a 0.8 nm layer of platinum using a Jeol JFC-2300 HR secondary vacuum metalliser. SEM investigations were carried out with a JEOL 7800 F field emission scanning electron microscope coupled with a Bruker energy dispersive analysis (EDS) system. This system is composed of two Bruker AXS 6|30 EDS detectors with a resolution of 126 eV (Kα line of Mn) at 20 kcps and an active surface of 30 mm^2 each. For both image acquisition and EDS analysis, an accelerating voltage of 15 kV, an electron current of 1.7 nA and a working distance of 9.5 mm between the sample and the last microscope lens are applied. Metallic copper is employed for energy calibration of the detectors and electron beam intensity measurement at the beginning of each session, while natural and synthetic minerals (albite, quartz, wollastonite, lead telluride) were used as standards. The Bruker Quantax Duo 400 analytical platform (Esprit software) served to deconvolve and quantify the EDS spectra. Localized point analyses of the inclusions were carried out for 50 s each.

2.2. Raman spectroscopy

Raman measurements were performed on the prepared samples using a LabRam Infinity (Jobin-Yvon-Horiba) Raman spectrometer. For our analyses, a 532 nm Nd:YAG laser source was used with a maximum power of 10 mW and a spectral resolution of 2.5 cm^{-1}. The instrument is combined with an Olympus BX-40 confocal microscope. At a magnification of 500× and area of 5 × 5 μm^2 is analysed at a depth of about 10 μm. A calibration on the silicon peak at 520 cm^{-1} was carried out before each set of data acquisitions (on average 10 per sample) with a laser aperture of 300 μm, an average acquisition time of 10 s, and repetitions of 10–30 times depending on the intensity of the spectrum. The spectral window chosen ranged from 60 cm^{-1} to 1570 cm^{-1}, with most of the signatures sought being between 100 cm^{-1} and 1000 cm^{-1}. The RRUFF database was used as a library of Raman spectra to identify the nature of the phases present by comparison (https://rruff.info/about/about_general.php).

2.3. LA-ICP-MS glass

Laser ablation inductively coupled plasma mass spectrometry (LA-ICP-MS) was undertaken at the Institut de Recherche sur les Archéomatériaux (IRAMAT-CEB) using a Resonetics M50E excimer laser and a Thermo Fischer Scientific ELEMENT XR mass spectrometer with a linear dynamic range of twelve orders of magnitude due to the combination of a dual-mode SEM and a Faraday detector. The laser operates at 193 nm, a 5 mJ energy and 10 Hz pulse frequency. The standard analytical protocol was used for all analyses that captures the signals in counts-per-second of 58 isotopes including major, minor, trace and rare earth elements. Each tessera was placed in a standard Resonetic S155 cell and ablated for 20 s pre-ablation and the acquisition of 9 mass scans over 27 s with a beam diameter between 50 μm and 100 μm and an argon/helium gas flow of 1 l/min Ar + 0.65 l/min He. ^{28}Si is used as internal standard, and external calibration is performed against Standard Reference Materials from the National Institute of Standards and Technology (NIST SRM) 610, the Corning reference glasses B, C, and D, as well as an archaeological glass sample (APL1) used for chlorine quantification. Reference materials Corning A and NIST SRM612 are analysed at regular intervals as unknowns to determine the accuracy and precision of the analyses (Table S2). The signals were converted into quantitative compositional data following the procedures detailed by Gratuze (2016).

2.4. LA-ICP-MS gold leaves

The analysis of the gold leaves by LA-ICP-MS was conducted in three different ways: in line mode on the surface of the gold leaf if a sufficiently large area was exposed (the minimum required is in the order of 1–2 mm^2), in line mode on the section of gold leaf between the support and the cartellina if a sufficient length of the leaf was accessible (the minimum required in the order of 1 mm), in spot mode, if the section of the gold leaf was only partially or patchily accessible between the support and the cartellina. From an analytical point of view, the analysis of the cross-sections in spot or in line modes ensured a more constant ablation and thus more stable and reproducible results than the analysis

on the surface of the gold leaf. However, contamination with elements such as copper, antimony or lead, which are also present in the glass, was more significant in the analysis of the sections, as the proportion of ablated glass was greater. In line mode, the quality of the ablation and thus the measured signal depended strongly on the thickness of the gold leaf and its adhesion to the glass.

The same parameters were used for the gold analyses as for the glass analyses (see above). Assuming no corrosion was present on the gold leaf, pre-ablation was reduced to 6 s before 25 mass scans were acquired for 12 isotopes ranging from copper to bismuth, over 22 s (isotopes measured were ^{63}Cu, ^{75}As, ^{105}Pd, ^{108}Pd, ^{109}Ag, ^{121}Sb, ^{193}Ir, ^{195}Pt, ^{197}Au, ^{202}Hg, ^{204}Pb and ^{209}Bi). For palladium, two isotopes were used to ensure that there was no interference from copper (ArCu at mass 105) or silver (peaks at masses 107 and 109). For surface analysis in line mode, the beam diameter was adjusted from 60 μm to 100 μm, while for section analysis in spot or line mode, the diameter was set at 50 μm to ensure both a good signal for gold and related elements and minimal contamination from the surrounding glass. ^{197}Au was used as an internal standard and external calibration was performed using industrially produced gold Standard Reference Materials. These are either Au–Ag–Cu alloys or high purity gold doped with a variety of trace elements at concentrations of 100–200 ppm or 15–30 ppm (RAuP3 and RAuP7, Rand Refinery Ltd, South Africa). In addition to these SRMs, ancient gold coins previously analysed by other methods (ICP-MS in liquid mode (Dussubieux and Van Zelst, 2004; Gratuze et al., 2004) were also used as reference materials (but the concentrations are not officially certified). Prior to processing, the acquisition spectra were systematically checked to remove any scans with insufficient signal for palladium, silver, platinum and gold (either: signal <10 x background or signal < average signal of the element/50). To avoid outliers in the contents of copper, antimony, lead and other elements that may also be present in the glass matrix, the compositions of the gold leaves were reduced and normalized to Au, Ag, Pd and Pt by weight (Table S3).

2.5. Statistical analysis

For the Principal Component Analysis (PCA) data were first reduced to the base glass oxides of Na, Mg, Al, Si, Cl, K, Ca, Ti, V, Cr, Mn, Fe, Rb, Sr, Y, and Zr, and normalized. PCA was then applied to a sub-set of elements (Ti, Al, Mg, Ca, Na, K, Cl, Cr, Rb, Sr, Y, Zr), using the standard PCA tool of Matlab that centres the data and uses the singular value decomposition (SVD) algorithm. Mn, Fe and V were omitted from the PCA to avoid distortions caused by colouring agents, while Cr was not found to contribute a discriminatory factor. The results of the first two principal components explain about 72.6% of the total variance of the dataset (Fig. 2).

3. Results

3.1. Compositional variability among the mosaic tesserae of the Umayyad Mosque in Damascus

Micro-destructive chemical analysis of 915 individual mosaic tesserae using LA-ICP-MS generated a large set of data (985 data points), where each measurement yielded analytical data of 58 chemical elements (see Materials and Methods, full dataset is given in data file S1). The compositional data reflect the mineralogy of the silica source (quartz-rich sands or pebbles) and the glassmaking recipe, whether mineral soda or plant ash was used as the main fluxing agent. 54 of the analysed tesserae show a plant ash composition with elevated plant ash related elements such as MgO, K_2O (Fig. 2A) and P_2O_5. The support of six gold leaf tesserae is of an alkali lead glass (data file S1). The high levels of additives, including lead, tin, antimony and arsenic, impede a clear classification of these 60 samples. It is reasonable to assume that these tesserae do not belong to the original early 8th-century mosaic decoration since no similar compositions are known from this period (Schibille, 2022; Schibille et al., 2020). Earlier Sasanian plant ash glass tends to have considerably higher MgO/CaO ratios, while higher heavy element contents would be expected from Egyptian productions (for a review see Schibille, 2022). It is likely that these tesserae derived from later restorations that are distinguishable by style and often identified by inscriptions (McKenzie, 2013; De Lorey, 1931). The overwhelming majority of the samples, however, are in line with natron-type glass typically encountered in the Mediterranean during the period of construction. Groupings within these natron glasses were established through an iterative and comparative process, taking into account especially elements associated with the silica source such as aluminium, calcium, titanium, zirconium and lanthanum and their relative abundance that in the past have been found to distinguish regional production groups (e.g. Ceglia et al., 2019; Degryse and Shortland, 2009; Freestone, 2020; Phelps et al., 2016; Schibille et al., 2019).

Principal component analysis (PCA) illustrates well the variability of the LA-ICP-MS dataset (Fig. 2A). The data were reduced to elements diagnostic of the base glass composition, normalized, and a PCA was then performed on a subset of these elements (Na, Mg, Al, Cl, K, Ca, Ti, Rb, Sr, Y, Zr). The first two principal components account for 72.6% of

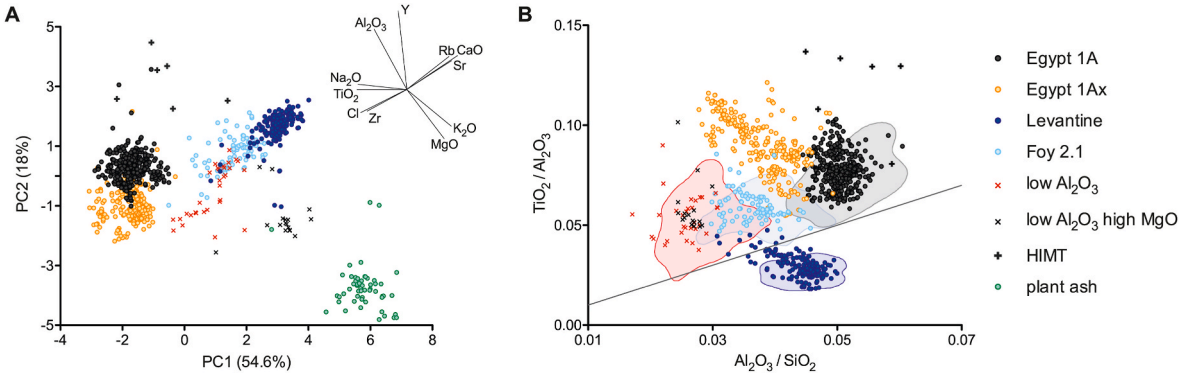

Fig. 2. Base glass characteristics of the mosaic tesserae from the Great Umayyad Mosque in Damascus. (A) Principal component analysis (PCA) of the reduced and normalized LA-ICP-MS dataset; the first two principal components (PC) represent 72.6% of the covariance and separate the dataset into 8 different base glass groups, vectors indicate direction and magnitude of the components; **(B)** Al_2O_3/SiO_2 versus TiO_2/Al_2O_3 distinguish different Egyptian and Levantine silica sources illustrated by the dividing line with a slope of 1, shaded outlines represent the 95% normal kernel density contours (using the online open access tool https://c14.arch.ox.ac.uk) of glass reference groups: Egypt 1A in grey (Schibille et al., 2019), Apollonia-type Levantine in dark blue (Brems et al., 2018; Freestone et al., 2008; Phelps et al., 2016), Foy 3.2 in red (Balvanović et al., 2018; Cholakova and Rehren, 2018; Foy et al., 2003; Gallo et al., 2014; Maltoni et al., 2015), Foy 2.1 in light blue (Ceglia et al., 2019; Foy et al., 2003; Schibille et al., 2016). (For interpretation of the references to colour in this figure legend, the reader is referred to the Web version of this article.)

variance and divide the data into 8 main compositional groups, the characteristics of which are indicated by the direction and length of the vectors (Fig. 2A). About 65% of the natron-type tesserae (n = 604) fall within two overlapping clusters (Egypt 1A & Egypt 1Ax), distinct from the other groups by higher Ti and Zr as well as higher soda and chlorine concentrations (Table 1). The two groups share a similar geochemistry, but their titanium, yttrium and especially their aluminium concentrations are sufficiently different to define them as two separate groups (Fig. 2A, Table 1). 19% of the natron base glasses (Levantine) have lower heavy element contents, lower soda levels and higher alkaline earth elements (e.g. Mg, Ca, Sr) and form a well-defined cluster. The rest of the tesserae are more variable and can be attributed to at least four additional compositional natron-type glass categories, including two low alumina types (Al_2O_3 < 2%), and an intermediate cluster (Foy 2.1) with slightly elevated titanium, zirconium and soda levels compared to Levantine glass. Six red and one gold leaf tesserae appear to correspond to so-called HIMT (high iron, manganese and titanium) glass.

The PCA model exemplifies the compositional variability of the analysed tesserae while highlighting the geochemical homogeneity of the majority of the samples belonging to Egypt 1A and Egypt 1Ax, which suggests that they represent material from the original 8th-century mosaic decoration. The relatively high number of Levantine samples means that these can be assumed to belong to the original mosaics, which may also be true for the other natron-type tesserae. They are consistent with older late antique glass groups, and probably represent reused and/or recycled material.

3.2. Comparison of the Damascus tesserae with known primary production groups

At the time the Umayyad mosque was built, the only known primary glass production sites using a mixture of evaporitic soda (natron) and quartz-rich sands were located in the coastal region of the Levant and in northern Egypt. The glassmaking furnaces at Apollonia-Arsuf on the Levantine coast are well-documented (Freestone et al., 2008; Tal et al., 2004); they were active in the 6th and 7th century CE and the chemical signature of the glass has been characterised in great detail (Freestone, 2020). The glassmaking activities at Bet Eli'ezer where the foundations of 17 tank furnaces were uncovered date probably to the late 7th and 8th century CE (Brems et al., 2018; Freestone et al., 2000, 2015; Gorin-Rosen, 1995, 2000). Contemporaneous with the construction of the Umayyad mosque in Damascus is the so-called Egypt 1A compositional group that has been identified based on the analysis of Islamic glass weights from Egypt (Gratuze, 1988; Gratuze and Barrandon, 1990). Egypt 1A is dated no later than the first quarter of the 8th century CE (Schibille et al., 2019).

Comparing the compositional fingerprints of the mosaic tesserae to these glass reference groups makes it possible to infer their likely provenance and chronological attribution. Despite the high variability of the alumina contents of the two main Egyptian tesserae groups, ranging from about 2% to 4% in the reduced and normalized composition, both groups exhibit distinctive heavy element traces that match the data of Egypt 1A glass weights. For there to be an acceptable correspondence between the elemental signature of the tesserae and the reference group, we introduced a threshold at 3.2% Al_2O_3 to subdivide the tesserae from Damascus (Fig. S2). The threshold was defined by the lowest alumina concentration of the glass weights with an Egyptian 1A composition (Schibille et al., 2019) minus the relative standard deviation derived from the aluminium measurements of Corning A (Table S2). The tesserae at the high end of the aluminium spectrum coincide perfectly with the Egypt 1A reference glass in terms of the Al_2O_3/SiO_2 as well as the TiO_2/Al_2O_3 ratios (Fig. 2B). No direct compositional match was found for the group with lower alumina contents (Al_2O_3 < 3.2%). This group was tentatively called Egypt 1Ax, because it shares a similar overall chemistry with Egypt 1A. All the trace and rare earth elements normalized to the upper continental crust lie perfectly within the concentrations limits of the Egyptian glass weights (Fig. 3). Given the geochemical similarities between the two groups of tesserae, it is highly likely that both groups were sourced from a similar, if not the same sand deposit in Egypt. If the aluminium content is linked to the clay fraction of the silica source, its concentration can vary according to the amount of clay without necessarily affecting the trace element patterns (Degryse and Shortland, 2009). The aluminium disparities could then be due to local variations in the distribution of minerals and the relative amount of clay as a result of different forces during sediment deposition (Brems et al., 2015, 2018).

On the same basis, it is clear that a very different silica source was exploited for the Levantine tesserae, which is reflected in their different trace element profile especially in relation to Ti, V, Cr, Zr, Nb, Hf and Ta (Fig. 3). To determine the most likely parent population of the Levantine group, the relative proportions of lime to alumina and soda to silica are compared (Fig. 4). This approach relies on the observation that there is a general decline in soda and increase in alumina concentrations in Levantine glass over the course of the first millennium CE (Freestone, 2020). One caveat is that the mosaic tesserae from Damascus contain various amounts of additives, particularly calcium phosphate as an opacifier, which can affect the CaO/Al_2O_3 ratios. Bearing this in mind, the Levantine tesserae are compared to data from the primary glass production sites at 4th-century Jalame (Brill, 1988, 1999), Apollonia-Arsuf probably 6th-to 7th-century (Brems et al., 2018; Freestone et al., 2008; Phelps et al., 2016), and late 7th-to 8th-century Bet'Eliezer (Brems et al., 2018; Freestone et al., 2000, 2015). The Levantine mosaic tesserae from Damascus are located at the interface between the Jalame and Apollonia reference groups dated to the period

Table 1
Average composition and standard deviations (σ) of the natron-type groups identified among the mosaic tesserae from the Great Mosque in Damascus. For comparability, data were reduced to the elements given and normalized to 100%.

	wt%											ppm				
	Na_2O	MgO	Al_2O_3	SiO_2	P_2O_5	Cl	K_2O	CaO	TiO_2	MnO	Fe_2O_3	B	Rb	Sr	Y	Zr
HIMT (n = 6)	15.2	1.37	3.38	64.0	0.38	1.03	0.98	8.08	0.40	1.21	3.83	163	8.06	680	12.0	175
σ	1.3	0.15	0.32	1.1	0.11	0.12	0.31	1.31	0.07	0.43	0.44	20	1.25	125	1.4	33
Foy 2.1 (n = 91)	17.8	1.00	2.40	66.1	0.13	0.86	0.63	8.01	0.14	1.53	1.19	154	7.68	644	7.50	79.6
σ	1.2	0.21	0.21	1.4	0.07	0.11	0.15	0.73	0.02	0.49	0.92	18	0.98	100	0.66	11.9
Al_2O_3 < 2% (n = 31)	19.7	0.65	1.72	67.6	0.08	1.09	0.41	7.23	0.09	0.73	0.58	149	5.73	521	6.21	50.7
σ	1.7	0.17	0.19	1.7	0.07	0.20	0.12	0.95	0.02	0.59	0.14	32	0.84	121	0.93	16.4
Al_2O_3 < 2% high Mg (n = 17)	15.1	1.32	1.81	68.1	0.37	0.78	1.32	8.29	0.11	0.40	2.28	120	6.08	561	5.24	53.9
σ	1.4	0.11	0.10	2.0	0.14	0.11	0.17	0.53	0.02	0.49	2.42	20	0.75	61	0.92	9.2
Levantine (n = 176)	14.4	0.67	2.96	67.6	0.18	0.78	0.85	9.57	0.09	1.20	1.59	92.6	11.6	478	7.23	46.0
σ	0.8	0.09	0.23	1.9	0.10	0.13	0.16	0.81	0.01	1.55	1.71	15.1	1.7	27	0.40	5.0
Egypt 1Ax (n = 251)	18.8	0.51	2.69	71.6	0.30	1.16	0.44	3.11	0.24	0.06	1.04	74.2	5.52	172	6.26	104
σ	1.0	0.07	0.31	1.7	0.29	0.13	0.08	0.82	0.03	0.10	0.44	12.4	0.73	73	0.62	16
Egypt 1A (n = 353)	18.6	0.65	3.51	69.7	0.28	1.11	0.49	3.60	0.27	0.17	1.50	74.1	7.25	219	7.13	103
σ	0.8	0.05	0.17	1.8	0.45	0.08	0.08	0.89	0.03	0.32	1.19	11.4	0.95	43	0.66	16

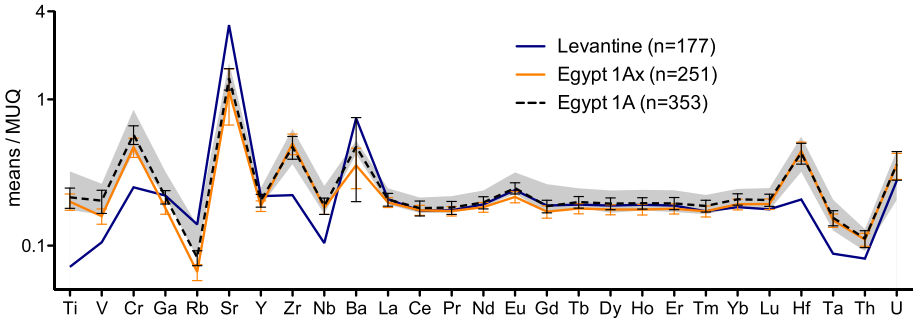

Fig. 3. Average trace element profile normalized to the relative abundance in the upper continental crust (Kamber et al., 2005) of the Egypt 1A, Egypt 1Ax and Levantine tesserae from Damascus. Shaded grey area defines the range of the glass reference group provided by the data of Egyptian glass weights (Schibille et al., 2019).

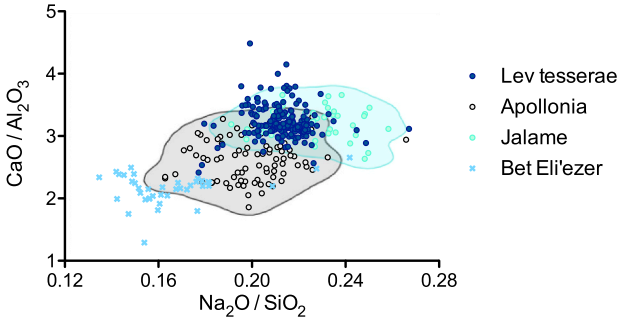

Fig. 4. Levantine type tesserae from the Great Mosque in Damascus compared to glass reference groups from Apollonia (Brems et al., 2018; Freestone et al., 2008; Phelps et al., 2016), Jalame (Brill, 1988, 1999) and Bet Eli'Ezer (Brems et al., 2018; Freestone et al., 2000, 2015). Jalame and Apollonia are outlined by 95% kernel density contours (using the online open access tool https://c14.arch.ox.ac.uk).

between the 4th to 7th century CE (Fig. 4). The late 7th to 8th-century glass from Bet'Eliezer can be excluded as a possible source.

All other natron-type tesserae from Damascus appear to be related to late antique base glass groups from Egypt (Fig. 2B). In terms of the silica source, the two low Al groups resemble Foy 3.2 glass (Foy et al., 2003), a 4th- and 5th-century glass categories (reviewed in Schibille, 2022). A common silica source is likely, although a sub-set of tesserae has zirconium values (~50 ppm) unusually low for Egyptian glasses (Table 1, dataset S1). There is considerable geochemical overlap between Foy 3.2 and Foy 2.1, a later 5th-to 6th-century Egyptian glass type (Barfod et al., 2020; De Juan Ares et al., 2019; Foy et al., 2003). Foy 3.2 has generally lower concentrations of alumina, lime, potassium and titanium than Foy 2.1, whereas the latter tends to contain higher background levels of recycling indicators (Ceglia et al., 2019). Defining a cut-off between these two late antique Egyptian glass groups is therefore necessarily arbitrary. This is especially true for mosaic tesserae, where the compositional spectrum is generally broader and often includes recycled material (Schibille et al., 2018). For the present purpose, the low Al group is defined on the basis of an aluminium content below 2%. The low Al high Mg group is distinguished by its elevated alkali and alkaline earth contents, especially Mg, Ca, and K as well as P (Table 1), which are markedly higher in the tesserae than in the late antique Foy 3.2 reference data. By inference, the low Al high Mg tesserae represent a variant of the Egyptian Foy 3.2 group that additionally contains a plant ash component. A similar phenomenon is known from so-called Magby glass, another Egyptian glass type that dates to the 6th and 7th centuries CE (Schibille, 2022; Schibille et al., 2016).

Our results show a clear dominance of Egyptian glass among the coloured tesserae (approximately 80%), most of which (Egypt 1A & 1Ax) are contemporaneous with the foundation of the Great Umayyad Mosque in Damascus. All other base glass types (low Al/Foy 3.2, Foy 2.1, Levantine) were in circulation prior to the 8th century. Whether these tesserae were simply re-used or whether glass was recycled and transformed into tesserae at the time of construction is difficult to say, not least because recycling is often not clearly visible in coloured and opaque glass. The conventional recycling indicators such as elevated transition metals, an increase in phosphorus, potash and/or lime, or loss of volatile elements such as soda and chlorine (Barfod et al., 2022) cannot be applied to glass that has been intentionally coloured and opacified, and processed at high temperatures for extended periods of time. Fiorentino (2021) has recently drawn parallels with 8th-century vessel glass, where there is a marked decline in Apollonia-type Levantine I, while Foy 2.1 is entirely absent (see also Phelps et al., 2016). It therefore appears more likely that the tesserae represent reused material collected from older mosaics or some storage facilities (Fiorentino, 2021; Shugar 2000).

In view of the difficulties in identifying recycling and reuse of strongly coloured tesserae, the gold leaf tesserae may serve as a proxy, since their base glass is not as extensively modified by additives. Gold leaf tesserae are made of two layers of glass (support and cartellina), between which a gold leaf is sandwiched. With few exceptions, the gold leaf tesserae from Damascus have remarkably high manganese contents (MnO >1.5%) that serve as an intentional colourant to obtain a variety of hues from greenish aqua to amber and black (data file S1) depending on the redox environment of the glass (Möncke et al., 2014). The effects of recycling vary between the different base glass types. Whereas the Levantine gold leaf tesserae display a linear increase in colourant-related elements (Sn, Cu, Pb), no close correlation is evident in the Foy 2.1 tesserae (Fig. S3 A-B). Instead, the Foy 2.1 gold leaf tesserae have heightened and positively correlated K_2O and P_2O_5 contents concomitant with a loss of soda and chlorine (Fig. S3 C-D), indicating repeated or prolonged heating and contamination of the glass by fuel vapour (Barfod et al., 2022; and references therein). The gold leaf tesserae of the low Al group ($Al_2O_3 < 2\%$) appear to be the least recycled glass, while higher magnesia concentrations in the low Al high MgO samples suggest the incorporation of an ash component. Whether this is due to contamination by fuel and vapours or the addition of soda-ash is not clear. Given the relative homogeneity of this group and the fact that sodium and magnesium show a slight positive trend, accidental contamination by fuel ash seems less likely. From these characteristics we may surmise that a large part of the gold leaf tesserae consists of recycled glass and/or reused tesserae. At what point these tesserae were made from recycled glass cannot be deduced from the glass composition alone. What is certain is that the base glasses of the gold leaf tesserae predate the construction of the mosque with the possible exception of one single sample that corresponds to the composition of Egypt 1A.

3.3. Compositional fingerprint of the gold leaf

It has previously been proposed that the composition of the gold leaf can provide additional clues about secondary working processes and help to distinguish between reused tesserae and freshly re-melted cullet turned into "new" tesserae because of a direct link with contemporary gold coinage (Neri et al., 2016). However, a comparison of the composition of the gold leaf of the tesserae from Damascus with Byzantine and early Umayyad coinage refutes any material connection. The gold content in the gold leaf tesserae from Damascus (72%–97%) is considerably lower and the silver levels are accordingly much higher than in both the Byzantine as well as the Umayyad gold coinage from Syria (Fig. 5A; Table S2), where a clear debasement of gold coinage and an increase in silver contents commenced only during the Abbasid caliphate (Gondonneau and Guerra, 2002; Jonson et al., 2014). The elevated silver concentrations of the gold leaf in comparison to gold coinage may be the result of the use of non-purified native gold (Gondonneau and Guerra, 2002; Jonson et al., 2014). Furthermore, the Pd/Au ratios of the gold leaves of essentially all Byzantine and Islamic mosaic tesserae differ significantly from those of the gold coinage (Fig. 5B). Pd/Au and Pt/Au ratios have been shown to be reliable markers for the identification of gold stocks as they do not appear to be affected by ancient metallurgical processes (Blet-Lemarquand et al., 2017). The compositional features of the gold leaf thus rules out the use of gold coins for the production of gold tesserae.

Incidentally, most Byzantine and Islamic tesserae from the 6th to 8th century CE included for comparative purposes (Hagia Sophia, Ephesus, Khirbet al-Minya) seem to derive from a common source of gold irrespective of the composition of the base glass, even though the absolute gold contents vary (Fig. 5, Table S2). The same type of gold was used for both Levantine and Egyptian Foy 2.1 tesserae. In contrast, the tesserae from the 4th-century Roman villa of Noheda (Spain) have much lower Pt/Au ratios, suggesting the exploitation of a very different gold source (Fig. 5B). These results confirm that secondary processing of late Roman tesserae in the western Mediterranean was different from Byzantine and early Islamic tesserae production in the east, both in terms of raw materials as well as secondary workshop locations. The characteristics of the gold leaves do not further constrain the geographical and/or chronological attribution of the tesserae from the Great Mosque in Damascus.

3.4. Colorants and opacifiers as indicators of secondary working techniques

Optical microscopy revealed that the mosaic tesserae have different degrees of opacity, ranging from transparent (gold leaf) to completely opaque depending on the amount of opacifying particles dispersed in the vitreous matrix (data file S1). Microstructural analyses of 30 mounted samples by SEM-EDS and Raman spectroscopy revealed two main opacifying techniques: *in situ* crystallisation, the addition of an opacifying pigment (*anime*), or a combination of the two. Nine macro colour groups (aqua, beige, black, blue, green, red, turquoise, yellow and yellowish green; Fig. S1, Table S1) have been classified that can be further refined into different shades (data file S1). In some cases, subtle variations are due to differences in composition, while in other cases, more complex compositional parameters and/or redox properties of the glass during processing may underlie the perceived nuances in colour.

Euhedral crystals of lead stannate ($PbSnO_3$), ranging in size from a few tens of nanometres to tens of microns, act as colourant and opacifier in the yellow, yellowish-green and green tesserae (Fig. 6A). Tin-based opacifiers have been widely used at least since the 4th century CE (Bonnerot et al., 2016; Freestone et al., 1990; Neri et al., 2017; Tite et al., 2008; Vandini and Fiorentino, 2020). The clear positive correlation of lead and tin especially in Egypt 1A and Egypt 1Ax demonstrates that the two components were added together in the form of a yellow pigment, which was obtained by mixing calcined metallic lead and tin with silica (Matin, 2019; Zecchin, 1989). This yellow pigment is typically added to a transparent glass at temperatures below 800 °C to avoid dissolution of the lead stannate. Lead stannate is frequently transformed into small secondary tin oxide particles (cassiterite, SnO_2) as well as lead-tin antimonate crystals (Fig. 6A). While lead stannate produces a lemon yellow, the presence of antimony modifies the hue to a more muted yellow (Verità et al., 2013). With increasing copper contents presumably in the form of Cu^{2+}, the colour shifts to a yellowish green and finally to a deep green. Without significant amounts of lead stannate, Cu^{2+} is responsible also for the colour of the turquoise tesserae that form the largest group in the collection, corresponding to the colour palette of the mosaics *in situ* (Fig. 1). It can be assumed that a higher Cu^{2+} content produces a deeper and darker turquoise, while elevated iron levels impart a greener tone.

Opacity of the aqua, beige and some turquoise tesserae results from the dispersion of calcium phosphate particles (hydroxyapatite $Ca_5(PO_4)_3(OH)$), which tend to transform around the edges into mixed sodium calcium phosphates (β-rhenanite $NaCaPO_4$; Fig. 6B) clearly identified as such by Raman spectroscopy. This reaction causes the formation of water vapour, which generates numerous bubbles throughout the glass, and an enrichment in calcium in the area surrounding the crystals, which leads to devitrification processes, the recrystallisation of wollastonite, as well as a certain degree of sodium depletion around the crystals (Maltoni and Silvestri, 2019; Silvestri et al., 2016; Verità et al., 2017). For this opacifying technology, bones were calcined at around 800 °C, the bone ash was then pulverised, mixed with glass and heated for 5–36 h (Maltoni and Silvestri, 2019). The use of calcium phosphate is known since the 5th century in the Levantine area, Asia Minor as well as northern Italy (Neri et al., 2017), and references therein; Vandini and Fiorentino, 2020). Regarding the

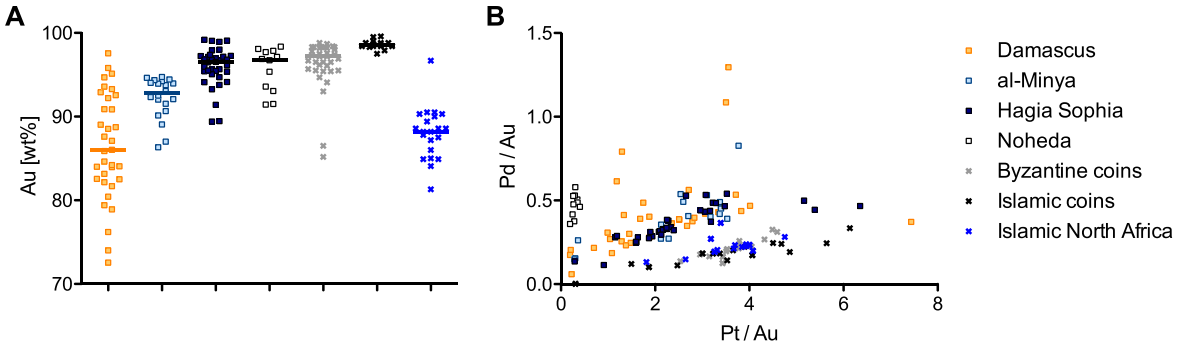

Fig. 5. Characteristics of the gold leaf of the Damascus tesserae. (**A**) Au contents of late Roman (Noheda), Byzantine (Hagia Sophia) and Islamic (Damascus, al-Minya) mosaic tesserae in comparison with Byzantine and Umayyad gold coinage (Byzantine, Islamic, Islamic North Africa) (Gondonneau and Guerra, 2002; Jonson et al., 2014); (**B**) Pd/Au versus Pt/Au ratios differentiate gold stocks and clearly distinguish the gold used for mosaics from that used in contemporary gold coinage. (For interpretation of the references to colour in this figure legend, the reader is referred to the Web version of this article.)

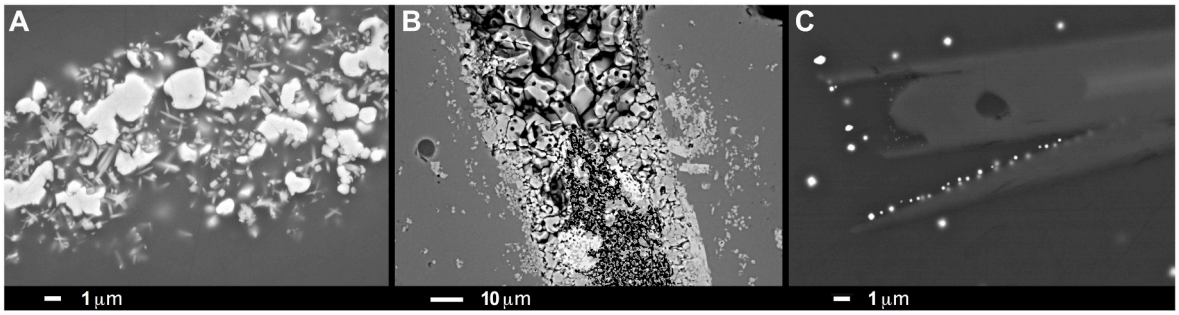

Fig. 6. Backscattered SEM images of mounted and polished cross sections. (**A**) Cassiterite crystals and lead stannate in green tessera (AFI 2295/47 AR001) of Egypt 1A composition; (B) particles of hydroxyapatite ($Ca_5(PO_4)_3OH$) surrounded by small particles of β-rhenanite ($NaCaPO_4$) in aqua-coloured Egypt 1A tesserae (AFI 2296/62 A003); (C) wollastonite crystals surrounded by copper nanoparticles in red tesserae (AFI 2295/67 Axx 003) with a Levantine base glass.

tesserae from Damascus, calcium phosphate was mostly used in combination with Egypt 1A and Egypt 1Ax glass and only sporadically with any of the other base glass groups (data file S1). A well-balanced ratio of Fe^{2+} and Fe^{3+} is responsible for the aqua colour (Schreurs and Brill, 1984), while in the beige tesserae iron is more oxidised in favour of Fe^{3+} due to the intentional addition of manganese oxide (MnO_2), of which inclusions have been detected by SEM and Raman spectroscopy.

In the red tesserae, nanoparticles of metallic copper have precipitated *in situ* which brings about a very intense red colouration due to a plasmon effect. No cuprous oxide (Cu_2O) was detected in the mounted samples by Raman spectroscopy or by SEM-EDS. From this and the fact that the red natron-type tesserae have relatively low copper and low lead concentrations we can extrapolate that metallic copper particles underlie most if not all of the red tesserae (Bandiera et al., 2020, 2021; Barber et al., 2009; Freestone, 1987; Freestone et al., 2003). The formation of metallic copper requires a strongly reducing atmosphere and/or the addition of reducing agents to the batch. The presence of magnetite and cassiterite in the polished cross sections suggests that iron and tin served as reducing agents either intentionally or accidently as part of the raw materials (Noirot et al., 2022). In all samples examined by SEM, the copper nanoparticles developed exclusively outside wollastonite crystals and often at the interface (Fig. 6C), which means that copper precipitated after the devitrification process of wollastonite that occurs at temperatures between 820 °C and 1050 °C (Barton and Guillemet, 2005). Hence, metallic copper nanoparticles developed necessarily at temperatures below 800 °C, most likely between 300 °C and 600 °C (Weyl, 1953).

For the other colours, our data show the use of cobalt (blue), medium to high levels of iron occasionally together with manganese and/or copper (black) and manganese oxide on its own in some black samples. Varying degrees of manganese are also present in many of the gold leaf tesserae. The support and cartellina of the gold leaf tesserae tend to have the same composition. There are a few exceptions where there is a notable difference in the manganese concentration, which was added to modify the colour of the glass (data file S1). Particularly interesting are those samples where the support and the cartellina are made of completely different base glasses. An extreme case in point is gold leaf tesserae NS078, the support of which is consistent with HIMT glass while the cartellina is of an $Al_2O_3 < 2\%$ composition. Similarly, sample NS060 combines a low alumina support with a Foy 2.1 cartellina. This is direct evidence for the contemporary processing of these different glass types in one and the same secondary workshop. Furthermore, these findings provide indirect evidence that these secondary workshops were located in Egypt, because the glasses that were combined are invariably of Egyptian provenance.

Thanks to the large quantity of analysed tesserae from the Great Mosque in Damascus, we can identify regional colour patterns. Aqua, black, green, turquoise and yellow tesserae were produced from all different base glasses (Levantine, Foy 2.1, Egypt 1A, Egypt 1Ax, low Al), more or less relative to the total number of samples in each group (Fig. 7). None of the cobalt blue specimens (Co > 200 ppm), and only one gold leaf tesserae are of the Islamic Egypt 1A or Egypt 1Ax base glass type, they all belong to the Levantine I, Foy 2.1 or the low Al groups. The copper red tesserae are predominantly made of a Levantine base glass, with the exception of a few HIMT, Foy 2.1 and low Al samples. The regional glass groups (Levantine, Egyptian) remain well defined and distinct, with no sign of extensive mixing between the two, suggesting independent secondary working. From this it can be inferred with some degree of certainty that the tesserae with an Egypt 1A or 1Ax signature were manufactured in Egypt and imported to Syria as finished or semi-finished products (i.e. coloured cakes) rather than in the form of raw glass.

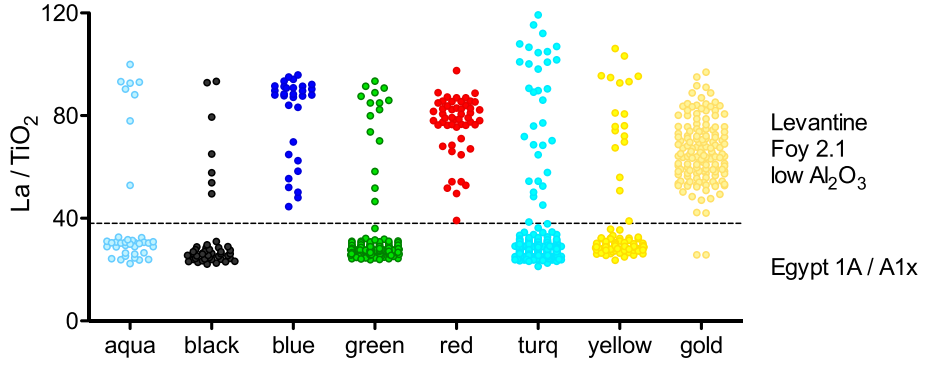

Fig. 7. Colour distribution as a function of the base glass reflected in the La/TiO_2 ratios. Horizontal line separates the 8th-century Egypt 1A and Egypt 1Ax base glass types from earlier glass groups and Levantine production groups. Tesserae with HIMT composition have been omitted for clarity. (For interpretation of the references to colour in this figure legend, the reader is referred to the Web version of this article.)

4. Discussion

The far-flung importation of large quantities of Egyptian glass tesserae to Damascus appears counterintuitive given the city's location near major glassmaking centres on the Levantine coast. It stands to reason that the Egyptian glass and mosaic industry was flourishing at the time, while Levantine glassmaking was already undergoing fundamental transformations. Problems in the Levantine glass industry have previously been suspected due to a decline in soda concentrations and an observed dominance of Egyptian imports of vessel glass into the Levant in the 8th century (Phelps et al., 2016). Significantly, the soda contents of the Egypt 1A and Egypt 1Ax tesserae from Damascus are on average 2 wt % higher than in the contemporary Egypt 1A reference group of early Islamic glass weights (Schibille, 2022). This shows that there was no shortage of soda for the production of glass tesserae destined for the mosaics of the Great Mosque of Damascus.

Our results further help to re-assess the production model of early Islamic mosaics. The manufacture of mosaic tesserae and glass inlays has a long history in Egypt (Nenna et al., 2000; Ritter, 2017; Van Lohuizen-Mulder, 1995, p. 208). In Byzantine mosaics from the 5th and 6th centuries, Egyptian base glasses such as HIMT and Foy 2.1 are typically more common than Levantine glass types (Freestone, 2020). Of the more than 300 analysed mosaic tesserae from the church of Hagia Sophia in Constantinople, for example, only about 5% correspond to a Levantine base glass, while the overwhelming majority are of a Foy 2.1 composition (unpublished data). These observations mark Egypt as a principal producer of mosaic tesserae during the late antique and early Islamic periods. Nonetheless, workshops specialising in tesserae-making must have existed in the Levant as well. Tesserae with a Levantine base glass are known from various late Roman (e.g. Schibille et al., 2018) and Byzantine contexts (Freestone et al., 1990; Neri et al., 2017; Schibille and McKenzie, 2014), occasionally indicating colour preferences. The selective use of Levantine glass for some colours in the mosaics of the Great Mosque of Damascus (cobalt blue, gold leaf, and red) is unlikely to be coincidental. A possible explanation is that some colours required access to exclusive raw materials (e.g. cobalt sources) or specialised know-how (gold leaf, copper red). Alternatively, some colours may have been more systematically collected and reused than others. If we take the 6th-century mosaic decoration of the church of Hagia Sophia in Constantinople as a point of reference for Byzantine mosaics, we find that the colours blue, red and gold predominate, while green is relatively rare and turquoise and yellow are completely absent (Schibille, 2013, 2014). The selective re-use of older blue, red and gold leaf tesserae could therefore be a question of availability. One possibility then is that some of these tesserae were retrieved from the Byzantine church that stood within the Damascene temenos prior to the foundation of the mosque (George, 2021). It is also conceivable that mosaic workshops were still active in the Levant in the late 7th or early 8th century. Given the apparent prevalence of Egyptian glass in Byzantine and Islamic mosaic decorations, however, it is presently unclear what the scale of Levantine tesserae production might have been.

What seems clear is that mosaic workshops operating in Egypt were in full swing throughout the late antique and into the early Islamic period, supplying major building projects first in the Byzantine Empire and later in the early Umayyad Caliphate. The mosaic tesserae from the early 8th-century caliphal palace at Khirbat al-Minya in Palestine, for example, have also been produced in Egypt (Adlington et al., 2020). Earlier samples from the Dome of the Rock (691–692 CE) as well as somewhat later tesserae from Khirbat al-Mafjar (724–743 CE) were similarly found to be of an Egypt 1 base glass (Fiorentino, 2021). The existence of secondary mosaic workshops in Egypt is also suggested by some gold-leaf tesserae, where there is a difference in composition between the support and cartellina, as they combine exclusively Egyptian base glass types (HIMT, Foy 2.1, low Al). A surge in monumental building campaigns at the end of the 7th and the beginning of the 8th century during the reigns of the Umayyad caliphs ʿAbd al-Malik (691/92 CE) and his son al-Walīd I (705–715 CE) dramatically increased the demand for architectural glass within a relatively short period of time (Leal, 2020). Early Islamic monuments such as the Great Mosque in Damascus are the visual representation of a new world order, a materialisation and visualization of Umayyad power and Muslim triumph (James, 2017, p. 263; Flood, 2001, pp. 214–216). Wall mosaics were part of this visual rhetoric to convey the political and economic power of the Umayyad caliphate and to demonstrate the capacity of the Umayyad dynasty to commandeer the necessary economic and material resources. Time was of the essence, and it is plausible that the manufacture and shipping of most of the material (about 65%) for the mosaics of the Great Umayyad Mosque was a direct commission. From the Aphrodito Papyrus (709–714 CE), an official correspondence between the governor of Egypt and the district prefect of Aphrodito, we know of a peremptory order to despatch forty skilled Egyptian workmen for the construction of the mosque at Damascus (Van Lohuizen-Mulder, 1995). This reflects the crucial role of the central government in the logistics of construction. Time constraints may also explain why the two contemporaneous Egyptian groups Egypt 1A and the newly identified Egypt 1Ax contain unusually high soda levels that exceed those of all other contemporary glasses so far analysed. The higher soda contents would have facilitated the processing of the glass mass and lowered the working temperature by an estimated 40 °C compared to the glass weights of an Egypt 1A composition according to the model of Fluegel (2007).

Secondary glass working processes are not immediately visible in the composition of the glass, and no archaeological evidence survives of first millennium mosaic workshops. The practices of mosaic making are therefore known only through a large-scale and comparative analytical approach of the material remains, which can reveal working practices and supply chains. The homogeneous material properties of the main group of tesserae from the Great Umayyad Mosque in Damascus substantiate a primary as well as secondary production in Egypt. Thus, our analytical data disprove Islamic textual sources (and modern scholarship alike) that for centuries have told and retold the story of the Byzantine origin of the materials. The mosaics are clearly not Byzantine but from Islamic Egypt and contemporary with the construction of the mosque.

Funding

This research was supported by the European Research Council Consolidator Grant ERC-2014-CoG [Grant Agreement No: 647315 to NS], and a Master 2 research grant by the Fondation des Sciences du Patrimoine [Grant No: AAP 2018].

Author contributions

Conceptualization: **NS, PL, IB, EB**, Methodology: **NS, PL, IB, LB, BG**, Investigation: **NS, PL, IB, LB, BG**, Visualization: **NS, LB**, Writing—original draft: **NS, IB, PL, BG**, Writing—revisions: NS, All data needed to evaluate the conclusions in the paper are present in the paper and/or the Supplementary Materials.

Declaration of competing interest

The authors declare that they have no known competing financial interests or personal relationships that could have appeared to influence the work reported in this paper.

Acknowledgments

We thank the members of the C2RMF, Anne Maigret, Clotilde Boust, Yvan Coquinot, Eric Laval and Thomas Calligaro for their technical support, and C.G. Specht for many helpful comments on the manuscript.

Appendix A. Supplementary data

Supplementary data to this article can be found online at https://doi.org/10.1016/j.jas.2022.105675.

References

Adlington, L.W., Ritter, M., Schibille, N., 2020. Production and provenance of architectural glass from the Umayyad period. PLoS One 15, e0239732.

Balvanović, R., Stojanović, M.M., Šmit, Ž., 2018. Exploring the unknown Balkans: Early Byzantine glass from Jelica Mt. in Serbia and its contemporary neighbours. J. Radioanal. Nucl. Chem. 317, 1175–1189.

Bandiera, M., Verità, M., Lehuédé, P., Vilarigues, M., 2020. The technology of copper-based red glass sectilia from the 2nd century AD Lucius Verus villa in Rome. Minerals 10, 875.

Bandiera, M., Verità, M., Zecchin, S., Vilarigues, M., 2021. Some secrets of Renaissance Venetian opaque red glass revealed by analyses and glassmaking treatises. Glass Technol. Eur. J. Glass Sci. Technol. 62, 24–33.

Barber, D.J., Freestone, I.C., Moulding, K.M., 2009. Ancient copper red glasses: investigation and analysis by microbeam techniques. In: Shortland, A.J., Freestone, I. C., Rehren, T. (Eds.), From Mine to Microscope: Advances in the Study of Ancient Technology. Oxbow Books, Oxford, pp. 115–127.

Barfod, G.H., Freestone, I.C., Lesher, C.E., Lichtenberger, A., Raja, R., 2020. 'Alexandrian'glass confirmed by hafnium isotopes. Sci. Rep. 10, 1–7.

Barfod, G.H., Freestone, I.C., Jackson-Tal, R.E., Lichtenberger, A., Raja, R., 2022. Exotic glass types and the intensity of recycling in the northwest Quarter of Gerasa (Jerash, Jordan). J. Archaeol. Sci. 140, 105546.

Barton, J., Guillemet, C., 2005. *Le Verre: Science et technologie*, Les Ulis. EDP Sciences.

Blet-Lemarquand, M., Nieto-Pelletier, S., Téreygeol, F., Suspène, A., 2017. Are platinum and palladium relevant tracers for ancient gold coins? Archaeometallurgical and archaeometric data to study an antique numismatic problem. Archaeometallurgy in Europe IV, Consejo Superior de Investigaciones Científicas, Bibliotheca Praehistorica Hispana 33, 19–28.

Bonnerot, O., Ceglia, A., Michaelides, D., 2016. Technology and materials of early Christian Cypriot wall mosaics. J. Archaeol. Sci.: Report 7, 649–661.

Brems, D., Pauwels, J., Blomme, A., Scott, R.B., Degryse, P., 2015. Geochemical heterogeneity of sand deposits and its implications for the provenance determination of Roman glass. Star: Science & Technology of Archaeological Research 1, 115–124.

Brems, D., Freestone, I.C., Gorin-Rosen, Y., Scott, R., Devulder, V., Vanhaecke, F., Degryse, P., 2018. Characterisation of Byzantine and early Islamic primary tank furnace glass. J. Archaeol. Sci.: Report 20, 722–735.

Brill, R.H., 1988. Scientific investigations of the Jalame glass and related finds. In: Weinberg, G.D. (Ed.), Excavations at Jalame: Site of a Glass Factory in Late Roman Palestine. University of Missouri, Columbia, pp. 257–291.

Brill, R.H., 1999. Chemical Analyses of Early Glasses. The Corning Museum of Glass, New York. Corning.

Ceglia, A., Cosyns, P., Schibille, N., Meulebroeck, W., 2019. Unravelling provenance and recycling of late antique glass from Cyprus with trace elements. Archaeological and Anthropological Sciences 11, 279–291.

Cholakova, A., Rehren, T., 2018. A late antique manganese decolourised glass composition: interpreting patterns and mechanisms of distribution. In: Rosenow, D., Phelps, M., Meek, A., Freestone, I. (Eds.), Things that Travelled: Mediterranean Glass in the First Millennium AD. UCL Press, London, pp. 46–71.

De Goeje, M.J., 2014. Aḥsan Al-Taqāsīm Fī Maʿrifat Al-Aqālīm by Al-Muqaddasī: Descriptio Imperii Moslemici/Auctore Schamso 'd-Din Abu Abdollah Mohammed Ibn Ahmed Ibn Abi Bekr Al-Banna Al-Basschari Al-Mokaddasi. In: (1906) by M.J. de Goeje. Brill. The Second Edition.

De Juan Ares, J., Guirado, A.V.-E., Gutiérrez, Y.C., Schibille, N., 2019. Changes in the supply of eastern Mediterranean glasses to Visigothic Spain. J. Archaeol. Sci. 107, 23–31.

De Lorey, E., 1931. Les mosaïques de la Mosquée des Omayyades à Damas, pp. 326–349. Syria.

Degryse, P., Shortland, A.J., 2009. Trace elements in provenancing raw materials for Roman glass production. Geol. Belg. 12, 135–143.

Dussubieux, L., Van Zelst, L., 2004. LA-ICP-MS analysis of platinum-group elements and other elements of interest in ancient gold. Appl. Phys. A 79, 353–356.

El-Cheikh, N.M., 2001. Byzantium through the Islamic prism from the twelfth to the thirteenth century. The Crusades from the Perspective of Byzantium and the Muslim World 53–70.

Finster, B., 1970. Die mosaiken der Umayyadenmoschee von Damaskus. Kunst Des. Orients 7, 83–141.

Fiorentino, S., 2021. A tale of two legacies: Byzantine and Egyptian influences in the manufacture and supply of glass tesserae under the Umayyad Caliphate (661-750 AD). Heritage 4, 2810–2834. https://doi.org/10.3390/heritage4040158.

Flood, F.B., 2001. The Great Mosque of Damascus: Studies on the Makings of an Ummayyad Visual Culture. Brill, Leiden, Boston, Cologne.

Fluegel, A., 2007. Glass viscosity calculation based on a global statistical modelling approach. Glass Technol. Eur. J. Glass Sci. Technol. 48, 13–30.

Foy, D., Picon, M., Vichy, M., Thirion-Merle, V., 2003. Caractérisation des verres de la fin de l'Antiquité en Méditerranée occidentale: l'émergence de nouveaux courants commerciaux. In: Foy, D., Nenna, M.-D. (Eds.), Échanges et commerce du verre dans le monde antique (Actes du colloque de l'AFAV, Aix-en-Provence et Marseille, 7-9 juin 2001). Éditions Monique Mergoil, Montagnac, pp. 41–85.

Freestone, I.C., 1987. Composition and microstructure of early opaque red glass. In: Bimson, M., Freestone, I.C. (Eds.), *Early Vitreous Materials*, British Museum Occasional Paper 56, pp. 173–191. London.

Freestone, I.C., 2020. Apollonia glass and its markets: an analytical perspective. In: Tal, O. (Ed.), *Apollonia-Arsuf Final Report of the Excavations, Volume II: Excavations outside the Medieval Town Walls*, Eisenbrauns. University Park, Pennsylvania, pp. 341–348.

Freestone, I.C., Bimson, M., Buckton, D., 1990. Compositional categories of Byantine glass tesserae. In: Annales du 11e Congrès de l'Association Internationale pour l'Histoire du Verre. Bâle, p. 11, 1988.

Freestone, I.C., Gorin-Rosen, Y., Hughes, M.J., 2000. Primary glass from Israel and the production of glass in late antiquity and the Early Islamic period. In: Nenna, M.-D. (Ed.), *La Route du verre. Ateliers primaires et secondaires du second millénaire av. J.-C. au Moyen Âge. Colloque organisé en 1989 par l'Association française pour l'Archéologie du Verre (AFAV)* Maison de l'Orient et de la Méditerranée, pp. 65–83. Lyon.

Freestone, I.C., Stapleton, C.P., Rigby, V., 2003. The production of red glass and enamel in the Late Iron Age, Roman and Byzantine periods. In: Entwistle, C. (Ed.), Through a Glass Brightly - Studies in Byzantine and Medieval Art and Archaeology Presented to David Buckton. Oxbow Books, Oxford, pp. 142–154.

Freestone, I.C., Jackson-Tal, R.E., Tal, O., 2008. Raw glass and the production of glass vessels at late Byzantine Apollonia-Arsuf, Israel. J. Glass Stud. 50, 67–80.

Freestone, I.C., Jackson-Tal, R.E., Taxel, I., Tal, O., 2015. Glass production at an early Islamic workshop in Tel Aviv. J. Archaeol. Sci. 62, 45–54.

Gallo, F., Marcante, A., Silvestri, A., Molin, G., 2014. The glass of the "Casa delle Bestie Ferite": a first systematic archaeometric study on late Roman vessels from Aquileia. J. Archaeol. Sci. 41, 7–20.

George, A., 2021. The Umayyad Mosque of Damascus: Art, Faith and Empire in Early Islam. Ginko Library, London.

Gómez-Morón, M.A., Palomar, T., Cerqueira Alves, L., Ortiz, P., Vilarigues, M., Schibille, N., 2021. Christian-Muslim contacts across the mediterranean: Byzantine glass mosaics in the great Umayyad Mosque of Córdoba (Spain). J. Archaeol. Sci. 129, 105370.

Gondonneau, A., Guerra, M.F., 2002. The circulation of precious metals in the Arab Empire: the case of the near and the Middle East. Archaeometry 44, 573–599.

Gorin-Rosen, Y., 1995. Hadera, Bet Eli'ezer. Excavations and Surveys in Israel 13, 42–43.

Gorin-Rosen, Y., 2000. The ancient glass industry in Israel – summary of the finds and new discoveries. In: Nenna, M.-D. (Ed.), *La Route du verre. Ateliers primaires et secondaires du second millénaire av. J.-C. au Moyen Âge. Colloque organisé en 1989 par l'Association française pour l'Archéologie du Verre (AFAV)* Maison de l'Orient et de la Méditerranée, pp. 49–63. Lyon.

Grafman, R., Rosen-Ayalon, M., 1999. The two great Syrian Umayyad mosques: Jerusalem and Damascus. Muqarnas 16, 1–15.

Gratuze, B., 1988. Analyse non destructive d'objets en verre par des méthodes nucléaires. PhD thesis. Application à l'étude des estampiles et poids monétaires islamiques. Université Orléans.

Gratuze, B., 2016. Glass characterization using laser ablation-inductively coupled plasma-mass spectrometry methods. In: Dussubieux, L., Golitko, M., Gratuze, B. (Eds.), Recent Advances in Laser Ablation ICP-MS for Archaeology, Series: Natural Science in Archaeology. Springer, Berlin, Heidelberg, pp. 179–196.

Gratuze, B., Barrandon, J.N., 1990. Islamic glass weights and stamps: analysis using nuclear techniques. Archaeometry 32, 155–162.

Gratuze, B., Blet-Lemarquand, M., Barrandon, J., 2004. Caractérisation des alliages monétaires à base d'or par LA-ICP-MS. Bulletin de la société française de numismatique. 59, 163–169.

James, L., 2017. Mosaics in the Medieval World: from Late Antiquity to the Fifteenth Century. Cambridge University Press, Cambridge.

Jonson, T., Blet-Lemarquand, M., Morrisson, C., 2014. The Byzantine mint in Carthage and the Islamic mint in north Africa. New metallurgical findings. Rev. Numis. 6, 655–699.

Kamber, B.S., Greig, A., Collerson, K.D., 2005. A new estimate for the composition of weathered young upper continental crust from alluvial sediments, Queensland, Australia. Geochem. Cosmochim. Acta 69, 1041–1058.

Leal, B., 2020. The Abbasid mosaic tradition and the great mosque of Damascus. Muqarnas 37, 29–62.

Maltoni, S., Silvestri, A., 2019. Investigating a Byzantine technology: experimental replicas of Ca-phosphate opacified glass. J. Cult. Herit. 39, 251–259.

Maltoni, S., Chinni, T., Vandini, M., Cirelli, E., Silvestri, A., Molin, G., 2015. Archaeological and archaeometric study of the glass finds from the ancient harbour of Classe (Ravenna- Italy): new evidence. Heritage Science 3, 13.

Matin, M., 2019. Tin-based opacifiers in archaeological glass and ceramic glazes: a review and new perspectives. Archaeological and Anthropological Sciences 11, 1155–1167.

McKenzie, J.S., 2013. Alexandria on the Barada: the mosaics of the great mosque in Damascus. In: Entwistle, C., James, L. (Eds.), New Light on Old Glass: Recent Research on Byzantine Mosaics and Glass. The British Museum Press, London, pp. 291–309.

Möncke, D., Papageorgiou, M., Winterstein-Beckmann, A., Zacharias, N., 2014. Roman glasses coloured by dissolved transition metal ions: redox-reactions, optical spectroscopy and ligand field theory. J. Archaeol. Sci. 46, 23–36.

Nenna, M.-D., Picon, M., Vichy, M., 2000. Ateliers primaires et secondaires en Egypte à l'époque gréco-romaine. In: Nenna, M.-D. (Ed.), La Route du verre. Ateliers primaires et secondaires du second millénaire av. J.-C. au Moyen Âge. Colloque organisé en 1989 par l'Association française pour l'Archéologie du Verre (AFAV). Maison de l'Orient et de la Méditerranée, Lyon, pp. 97–112.

Neri, E., Verità, M., Biron, I., Guerra, M.F., 2016. Glass and gold: analyses of 4th–12th centuries Levantine mosaic tesserae. A contribution to technological and chronological knowledge. J. Archaeol. Sci. 70, 158–171.
Neri, E., Jackson, M., O'hea, M., Gregory, T., Blet-Lemarquand, M., Schibille, N., 2017. Analyses of glass tesserae from Kilise Tepe: new insights into an early Byzantine production technology. J. Archaeol. Sci.: Report 11, 600–612.
Noirot, C., Cormier, L., Schibille, N., Menguy, N., Trcera, N., Fonda, E., 2022. Comparative Investigation of Red and Orange Roman Tesserae: the Role of Cu and Pb in Colour Formation. Heritage.
Phelps, M., Freestone, I.C., Gorin-Rosen, Y., Gratuze, B., 2016. Natron glass production and supply in the late antique and early medieval Near East: the effect of the Byzantine-Islamic transition. J. Archaeol. Sci. 75, 57–71.
Qaddumi, G.H., 1996. Book of Gifts and Rarities: Selections Compiled in the Fifteenth Century from an Eleventh-Century Manuscript on Gifts and Treasures = (Kitāb Al-Hadāyā Wa Al-Tuḥaf), vol. 29. Harvard Middle Eastern Monographs, Harvard.
Ritter, M., 2017. Der umayyadische Palast des 8. Jahrhunderts in Ḫirbat al-Minya am See von Tiberias: Bau und Baudekor. Reichert Verlag, Wiesbaden.
Schibille, N., 2013. A quest for wisdom: the sixth-century mosaics of Hagia Sophia in Constantinople and late antique aesthetics. In: Entwistle, C., James, L. (Eds.), New Light on Old Glass: Recent Research on Byzantine Glass and Mosaics. British Museum Research Publications, London.
Schibille, N., 2014. Hagia Sophia and the Byzantine Aesthetic Experience. Aldershot.
Schibille, N., 2022. Islamic Glass in the Making: Chronological and Geographical Dimensions. Leuven University Press, Leuven.
Schibille, N., Gratuze, B., Ollivier, E., Blondeau, É., 2019. Chronology of early Islamic glass compositions from Egypt. J. Archaeol. Sci. 104, 10–18.
Schibille, N., Ares, J.D.J., García, M.T.C., Guerrot, C., 2020. Ex novo development of lead glassmaking in early Umayyad Spain. Proc. Natl. Acad. Sci. USA 117, 16243–16249.
Schibille, N., Neri, E., Ebanista, C., Ammar, M.R., Bisconti, F., 2018. Something old, something new: the late antique mosaics from the catacomb of San Gennaro (Naples). J. Archaeol. Sci.: Report 20, 411–422.
Schibille, N., McKenzie, J., 2014. Glass tesserae from Hagios Polyeuktos, Constantinople: their early Byzantine affiliations. In: Keller, D., Price, J., Jackson, C. (Eds.), Neighbours and Successors of Rome: Traditions of Glass Production and Use in Europe and the Middle East in the Later 1st Millennium AD. Oxbow Books, Oxford, pp. 114–127.
Schibille, N., Meek, A., Tobias, B., Entwistle, C., Avisseau-Broustet, M., Da Mota, H., Gratuze, B., 2016. Comprehensive chemical characterisation of Byzantine glass weights. PLoS One 11, e0168289.
Schreurs, J.W., Brill, R.H., 1984. Iron and sulfur related colors in ancient glasses. Archaeometry 26, 199–209.
Shugar, A.N., 2000. Byzantine opaque red glass tesserae from Belt Shean, Israel. Archaeometry 42, 375–384.
Silvestri, A., Nestola, F., Peruzzo, L., 2016. Multi-methodological characterisation of calcium phosphate in late-Antique glass mosaic tesserae. Microchem. J. 124, 811–818.
Tal, O., Jackson-Tal, R.E., Freestone, I.C., 2004. New evidence of the production of raw glass at late Byzantine Apollonia-Arsuf, Israel. J. Glass Stud. 46, 51–66.
Tite, M., Pradell, T., Shortland, A., 2008. Discovery, production and use of tin-based opacifiers in glasses, enamels and glazes from the late Iron Age onwards: a reassessment. Archaeometry 50, 67–84.
Van Lohuizen-Mulder, M., 1995. The mosaics of the great mosque at Damascus. BABESCH Annual Papers on Mediterranean Archaeology 70, 193–213.
Vandini, M., Fiorentino, S., 2020. From crystals to colour: a compendium of multi-analytical data on mineraological phases in opaque coloured glass mosaic tesserae. Minerals 10. https://doi.org/10.3390/min10070609.
Verità, M., Santopadre, P., De Palma, G., 2017. Scientific investigation of glass mosaic tesserae from the 8th century AD archaeological site of Qusayr'Amra (Jordan). Bollettino ICR - Nuova Serie 32, 7–18.
Verità, M., Maggetti, M., Saguì, L., Santopadre, P., 2013. Colors of Roman glass: an investigation of the yellow sectilia in the Gorga collection. J. Glass Stud. 55, 39–52.
Weyl, W.A., 1953. Coloured Glass. Society of Glass Technology, Sheffield.
Zecchin, L., 1989. *Vetro e vetrai di Murano : studi sulla storia del vetro* Venice: Arsenale.